Available online at www.sciencedirect.com

ScienceDirect

IFAC Papers Online CONFERENCE PAPER ARCHIVE

IFAC-PapersOnLine 48-19 (2015) 112–117

A Polyurethane-based Compliant Element for Upgrading Conventional Servos into Series Elastic Actuators ⋆

Leandro Tomé Martins * **Christopher A. Arend Tatsch** *
Eduardo Henrique Maciel ** **Reinhard Gerndt** ***
Rodrigo da Silva Guerra *

* *Univ. Federal de Santa Maria, RS, Brazil (e-mail:rodrigo.guerra@ufsm.br).*
** *Univ. Federal do Rio Grande do Sul, RS, Brazil (e-mail:eduardo.maciel@ufrgs.br)*
*** *Ostfalia Univ. of Applied Sciences, Wolfenbttel, Germany (e-mail:r.gerndt@ostfalia.de)*

Abstract: This paper presents a novel compliant spring system designed to be attached to a conventional robotics servo motor, turning it into a series elastic actuator (SEA). The system is composed by only two mechanical parts: a torsional polyurethane spring and a round aluminum support for link attachment. The polyurethane spring, had its design derived from a iterative FEM-based optimization process. A magnetometer based circuit is used to measure angular displacement and communicate it through a RS485 bus protocol.

Keywords: robotics, passive compliance, modular design, series elastic actuator

1. INTRODUCTION

Traditional robot manipulators, such as the ones designed for use in controlled industrial settings, typically use very stiff joints, heavy and rigid structures and powerful actuators. These robots usually operate at a low speed and with high torque, demanding large peak power output for short periods, accurate feedback sensing, and suitability in shape, size and mass (Wyeth, 2006). With the advances on fast and powerful controllers and precise sensors, the demand for such decoupling between a manipulator and its load can be relaxed without compromising the performance. Moreover, the demands of the field of human-robot interaction rises concern on the safety of the actuation mechanism and on its behaviour towards uncertainties in the environment.

The solutions for adding compliance into the design of robot joints can be divided in two groups: (1) active (or simulated) compliance and (2) passive (or real) compliance. Simulated compliance is achieved through software, by continuously controlling the impedance of back-drivable electric motors (see for instance Jain and Kemp (2010)). Real or passive compliance is achieved by inserting a elastic element between the motor and load. This is typically done through the use of mechanical springs in the design of the joints (see for instance Guizzo and Ackerman (2012)).

A Series Elastic Actuator (Pratt and Williamson, 1995) basically consists of traditional stiff servo actuator in series with a spring connected to the load, as shown in

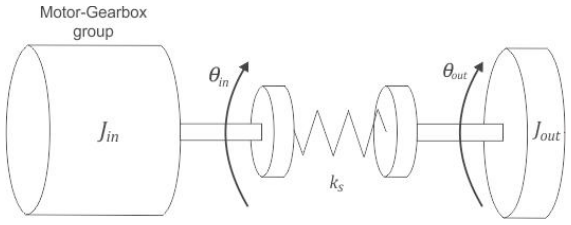

Fig. 1. Series Elastic Actuator Topology (Laffranchi et al., 2011)

Figure 1. This topology allows the load to be partially decoupled from the motor, and the force exerted on the output of the compliant element can be evaluated by simply measuring the deflection of this component. Carpino et al. (2012) splits the existing SEAs design in two classes. The first class comprises compliant systems adopting helicoidal compression springs arranged in such a way that a centering elastic torque is produced when the joint shaft is rotated (see Fig.2-*A* presented by Tsagarakis et al. (2009) and Fig.2-*B* presented by Yoon et al. (2003)). The second class includes compliant systems employing torsional springs somehow connected to the load (see for instance Fig.2-*C* and Fig.2-*D* presented by Carpino et al. (2012) and dos Santos and Siqueira (2014), respectively).

These designs are complex and difficult to manufacture. The helicoidal spring designs usually require an elevate number of parts, and the torsional spring designs in the literature use expensive alloys that have to be milled. In both cases the resulting SEA becomes rather heavy and bulky. These springs are not suitable for the ever growing market of smaller humanoid robots or other robots

⋆ This work was partially funded by Univ. Federal de Santa Maria, by Ostfalia Univ. of Applied Sciences and by the RoboCup Federation.

10.1016/j.ifacol.2015.12.019

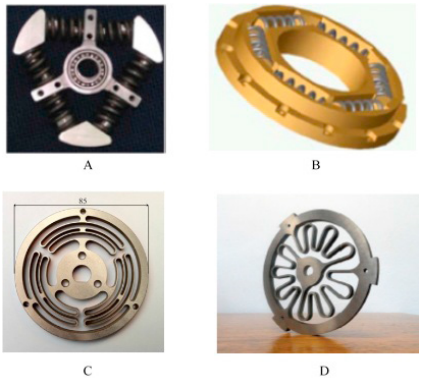

Fig. 2. Examples of existing compliant elements. Laffranchi et al. (2011)

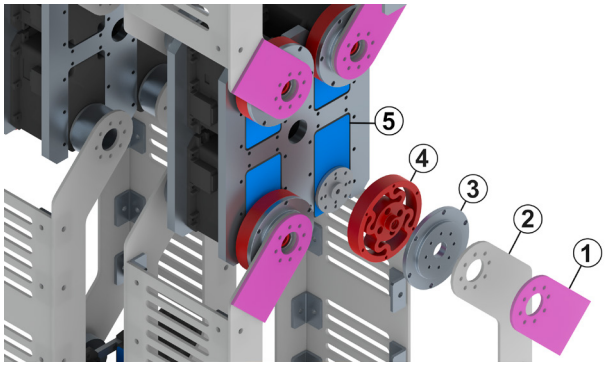

Fig. 4. Knee joint assembly with four SEA, including exploded view. The components are: (1) circuit board, (2) leg link frame, (3) attachment cover, (4) polyurethane torsional spring, (5) Dynamixel MX-106 servo actuator. Drawn by Eduardo Henrique Maciel.

Fig. 3. Polyurethane-based spring used in our system

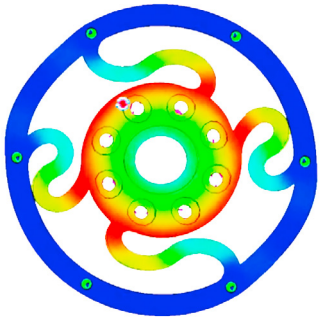

Fig. 5. Finite Element Analysis showing the maximum displacement region in red.

based on traditional consumer servos such as the Robotis Dynamixel MX line of actuators.

In previous work (see Martins et al. (2014)) the authors of this paper have experienced with the design of a SEA module using helicoidal springs. The observed disadvantages included insertion of extra friction and non-linearities, backlash and assembly complexity. Thus, from this previous experience we came up the idea to design a new compliant element based on an alternative material, avoiding helicoidal springs and numerous other parts.

The design consists of a two-part component, using a modular polyurethane-based spring. This is an low-cost design that can be easily manufactured using a CNC router. Our aim is toward applications on lower budget humanoid robots, trying to provide a better support for impact on the knees during walking and protecting shoulder joints during a fall. Our designed device consists of software, firmware, electronics and a mechanical accessory that can be easily attached to the popular Dynamixel MX series servo actuators, manufactured by Robotis, transforming it into a SEA. However the general idea could be easily adapted to fit most servo actuators of similar “RC-servo-style” design.

The remainder of this work is organized as follows: Section 2 explains the main details regarding the design as well as the modelling of the SEA. Section 3 shows some data regarding the actual construction of the device and a robot upgrade case. Section 4 presents the closing remarks and future work.

2. METHODOLOGY

2.1 Design Requirements

The elastic element presented in this paper was designed aiming the application on the knees of a humanoid robot which uses a parallel leg mechanism. This robot is being developed by the joint RoboCup team WF Wolves (Germany) & Taura Bots (Brazil) (Hannemann et al., 2014). This robot employs the Dynamixel MX-106 servo actuators manufactured by Robotis in a redundant arrangement, allowing the springs to be compressed against each other for leg rigidity modulation (see Figure 4).

The SEA design was elaborated to ensure a symmetrical response in both directions, without saturation when exposed to the maximum torque supported by the motor. The spring consists on four ”s” shapes, with the width of 3mm. This dimension was decided after a CAD based Finite Element Analysis (see Figrue 5)

2.2 Manufacture

The manufacturing of the two mechanical parts was all done on an ordinary 3-axis CNC router, using a 2mm cutter. Both the polyurethane and the aluminum parts can be milled in a single operation, without the need for fixing the part in different orientations. Refrigeration fluid is not needed.

2.3 System Identification and Control

The open-loop SEA system shown in Figure 6 is composed by an input signal, an output signal, a disturbance signal and two transfer functions. One transfer function corresponds to the dynamics of the servo motor, which combines the behaviors of its internal PID controller, its DC motor driver and the DC motor inside its case. From the command of a desired position $\theta_m{}^*$, an error signal is intrinsically compensated by a PID controller and then converted into voltage level to the motor armature generating θ_m. The other transfer function corresponds to the compliant element behaviour, which has, as input, an external load τ_L, and produces a angular deflection $\Delta\theta$. The output of the SEA system, is the final position θ_f, given by the sum $\theta_m + \Delta\theta$. The external load can be seen as a disturbance to the system.

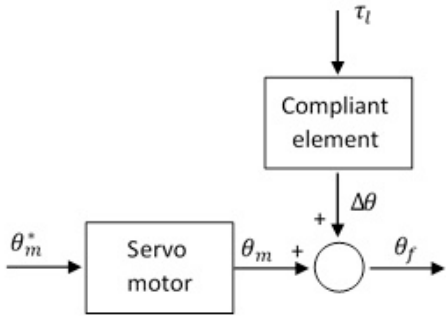

Fig. 6. Typical impedance control loop.

In order to find the theoretical SEA model, we present a system identification method based on *Matlab System Identification Toolbox*, and then a control law is presented. The controller has the goal of providing the final position to track the desired position, even under the effect of an external load.

2.4 Electronics

In order to read the spring's angular displacement a magnet/magnetometer based circuit was designed (see Figure 7). A radially polarized cylindrical rare earth magnet is placed on the center of the polyurethane part, and the circuit board is placed on top of the assembly so that the magnetometer chip is aligned with it. For educational purposes the electronics was designed to be Arduino compatible. The firmware mimics Dynamixel's protocol: an id is assigned to each SEA, as if these were additional torque-disabled servo-motors, answering queries about their angular positions on the same RS485 bus.

2.5 ARX model derivation and Least-squares estimator

Here we assume the system can be reasonably approximated by a general linear polynomial model. In this paper, an Auto-Regressive with External Input (ARX) model structure is chosen to represent the SEA system (Ljung, 1987). The algorithm involved in the ARX model estimation is fast and efficient when the number of data points is very large. This model structure is a derivation of generic model from equation (1), and its representation is in the form:

$$\begin{aligned} &y(t) + a_1 y(t-1) + ... + a_{na} y(t-na) \\ &= b_1 u(t-1) + ... + b_{nb} u(t-nb) + e(t) \end{aligned} \tag{1}$$

where the adjustable parameters are in this case

$$\psi = [\, a_1 \ ... \ a_{na} \ b_1 \ ... \ b_{nb} \,]^T \tag{2}$$

If we introduce

$$A(q) = 1 + a_1 q^{-1} + ... + a_{na} q^{-na} \tag{3}$$

and

$$B(q) = 1 + b_1 q^{-1} + ... + b_{nb} q^{-nb} \tag{4}$$

where the shift operator q is given by

$$qu(t) = u(t+1) \tag{5}$$

and the backward shift operator q^{-1} is given by

$$q^{-1} u(t) = u(t-1) \tag{6}$$

we see that from (1), the term $e(t)$ corresponds to

$$\frac{y(t)}{u(t)} = G(q, \psi) = \frac{B(q)}{A(q)} \tag{7}$$

Computing the one-step-ahead prediction, the predictor for (1) gives

$$\hat{y}(t, \psi) = \psi^T \varphi(t) = \varphi^T(t) \psi \tag{8}$$

The predictor is a scalar product between a known data vector $\varphi(t)$ and the parameter vector ψ. Such a model is called *linear regression* in statistics, and the vector is known as the regression vector, obtained through measurements and given by

$$\varphi(t) = [\, -y(t-1) \ ... \ -y(t-na) \ u(t-1) \ ... \ u(t-nb) \,]^T$$

With (8), the predictor error becomes

$$\varepsilon(t, \psi) = y(t) - \varphi^T(t) \psi \tag{9}$$

and the criterion function (or cost function) is given by

$$V(\psi, Z^n) = \frac{1}{N} \sum_{t=1}^{N} \frac{1}{2} [y(t) - \varphi^T(t) \psi]^2 \tag{10}$$

where $Z^n = [y(1), u(1), y(2), u(2), ..., y(N), u(N)]$ is the collected batch of data from the system. The problem to be solved here is decide upon how to use the information contained in Z^n to select a proper value $\hat{\psi}_N$ of the parameter vector.

Therefore the *least-squares criterion* (10) for the linear regression (8) can be minimized analytically, provided the indicated inverse exists, by

$$\begin{aligned} &\hat{\psi}_N^{LS} = argmin V_N(\psi, Z^N) \\ &= [\frac{1}{N} \sum_{t=1}^{N} \varphi(t) \varphi^T(t)]^{-1} \frac{1}{N} \sum_{t=1}^{N} \varphi(t) y(t) \end{aligned} \tag{11}$$

the least-squares (LS) estimate.

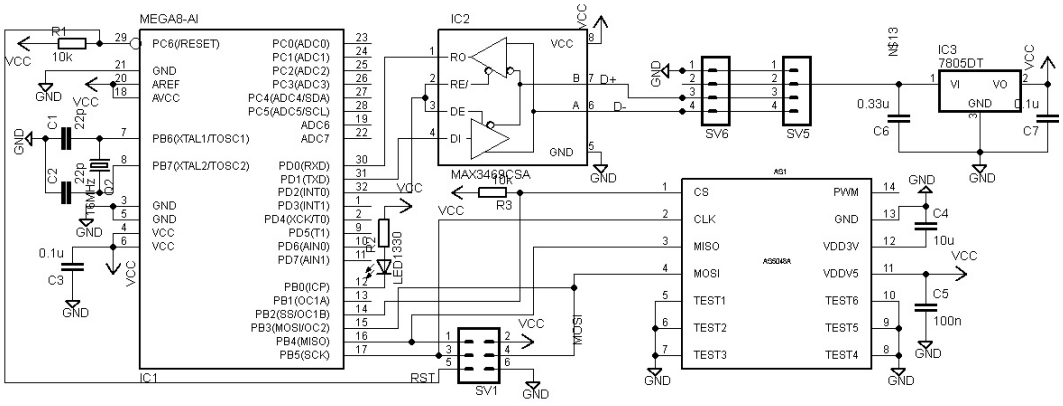

Fig. 7. Schematic of the instrumentation electronics on the SEA.

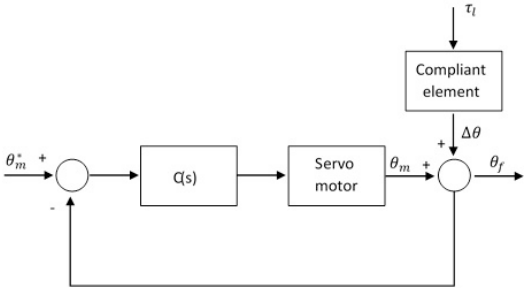

Fig. 8. Typical impedance control loop.

2.6 Controller

The controller is designed in order to let the final position θ_f track the set-point position θ_m^* of the servo motor. The closed-loop system is shown in Figure 16. Another goal of the compensated system is to reject disturbances. A discrete PID controller was used, since this is a simple method to match the specifications of project, and the control law is given by

$$\begin{aligned} u(k) &= K_P e(k) + K_I \frac{T_s}{2}\frac{q+1}{q-1}e(k) K_D \frac{q-1}{T_s q}e(k) \\ &= (K_P - \frac{K_I T_s}{2})e(k) + (K_I T_s)\sum_{j=0}^{k} e(j) \\ &\quad + \frac{K_D}{T_s}[e(k) - e(k-1)] \\ &= K_{P(digital)} e(k) + K_{I(digital)} \sum_{j=0}^{k} e(j) \\ &\quad + K_{D(digital)}[e(k) - e(k-1)] \end{aligned} \tag{12}$$

where q is the one-step advance operator, T_s is the sample time, $K_P, K_I and K_D$ are the gains to be determined. $e(k)$ is the error between the output (final position) and the input (set-point position) of the system.

3. RESULTS

3.1 Obtaining the stiffness

For a linear spring, the torsional stiffness k can be described by Hooke's law, given by

$$\tau = -k.\Delta\theta \tag{13}$$

In order to assess the stiffness of the spring known mass was applied on the tip of the frame attached to the compliant element output, and measuring the resulting angle deflection $\Delta\theta$. The rotational torque derived from the known mass can be determined by

$$\tau = Fl = mgl\cos(\Delta\theta) \tag{14}$$

These process was repeated for 20 different values of mass and the the results were plotted, as shown in Figure 9.

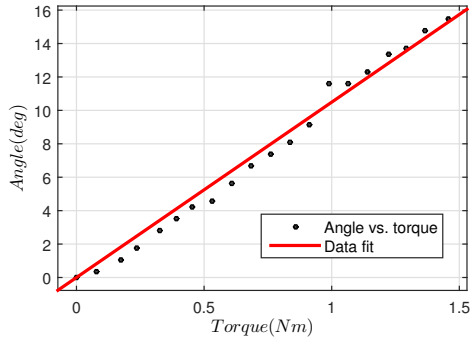

Fig. 9. Linear regression of experiment data set.

A line which fits the data set was estimated by a linear regression method. Thus, given that the line equation is $y = p_1 x + p_2$, the coefficients found for this line were $p_1 = 10.49$ and $p_2 = 0$, as shown in Figure 9. The slope of this line represents the inverse of the stiffness, so, the value for the torsional stiffness k is

$$k = \frac{1}{10.49} = 0.09 Nm/deg \tag{15}$$

3.2 Obtaining the transfer function of the compliant element system

In order to raise the transfer function for the compliant element behaviour, a step response experiment was performed. The step signal input was the torque applied on the compliant element output by releasing a known weight hanging on the frame and measuring the angle deflection of the compliant element. For this experiment, the motor was kept stationary, and the angle deflection was just produced by the compliant element. The step response for the real system is shown in Figure 10.

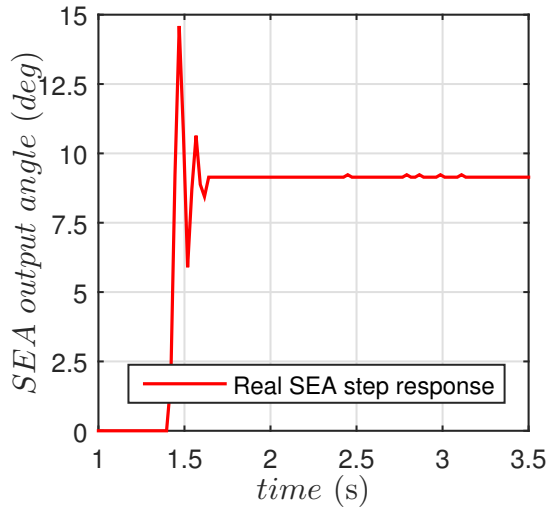

Fig. 10. Step response for the real SEA system.

The output behaves as a spring with a high damping constant. In order to identify the transfer function, the system identification method explained previously was used. We applied an optimization process using *Matlab System Identification Toolbox* to identify which ARX model better fits the data set. The transfer function that better fitted the experimental data was

$$G(z) = \frac{8.431z}{z^2 - 0.743z + 0.4229} \tag{16}$$

Figure 11 shows the step response for the identified transfer function.

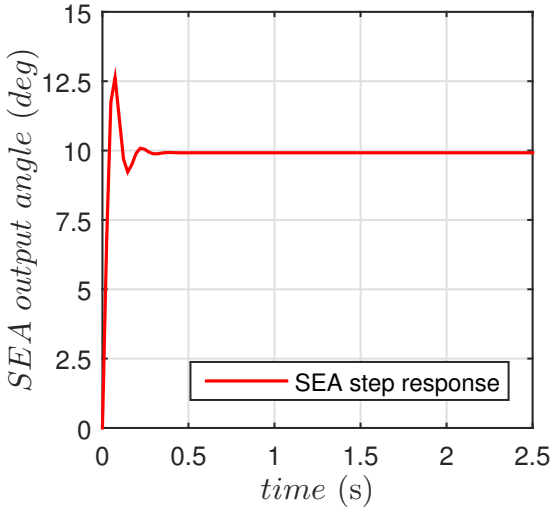

Fig. 11. Step response for the simulated SEA system.

3.3 Obtaining the transfer function of the servo motor

Similarly to the method described in the previous subsection, a reference signal (desired position) was applied to the servo motor, and the output signal (servo motor position) was measured in order to obtain the step response for the system, Figure 12. By the step response, an ARX identification method was performed and the transfer function for the Dynamixel servo motor was found. The transfer function equation obtained by this identification method is

$$G(z) = \frac{0.03044z^2}{z^3 - 1.774z^2 + 0.865z - 0.06091} \tag{17}$$

This is a discrete-time transfer function with a sample time of $T_s = 24.49ms$. In order to validate system transfer function, its open-loop step response was also plotted. The Figure 13 shows the step response for the transfer function of equation (17). The amplitude of the step response is 90, in order to mimic a valid angle for the motor.

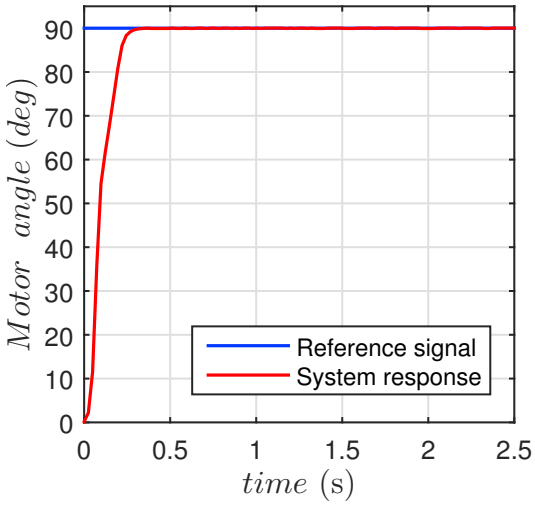

Fig. 12. Step response for real dynamixel motor.

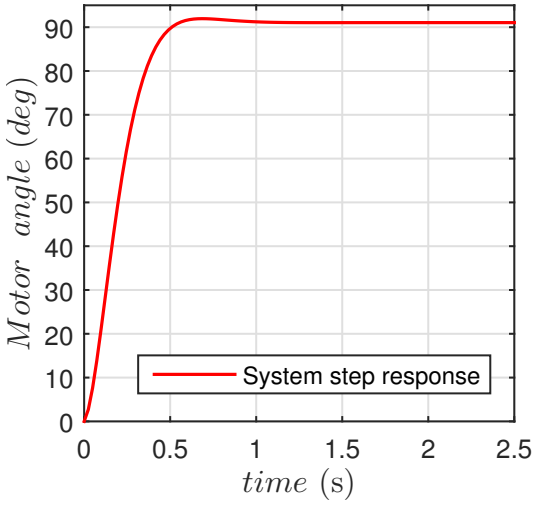

Fig. 13. Step response for simulated dynamixel motor.

3.4 Controller

Once the transfer functions of both servo motor system and compliant element system were found, the system could be simulated. To evaluate the uncompensated system behaviour, an angle reference of 90 degrees was set and after a 3 seconds delay, an external load of $1Nm$ was applied, resulting in a steady state error as depicted in Figure 14.

Finally, a PID control was implemented, as seen in Figure 15, with its respective response shown in Figure 16.

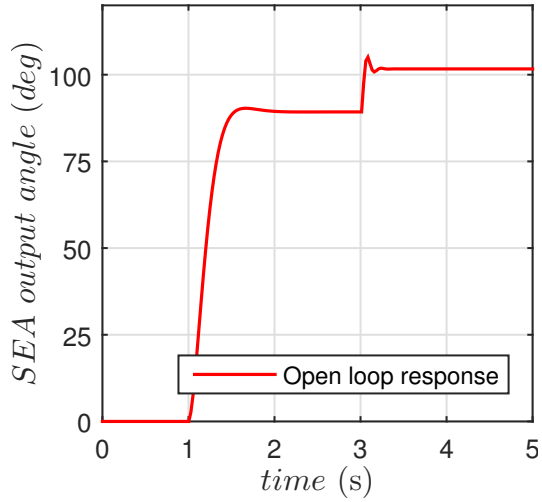

Fig. 14. The uncompensated system shows an steady state error when load is applied.

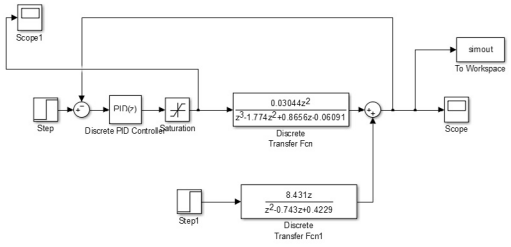

Fig. 15. Compensated SEA system

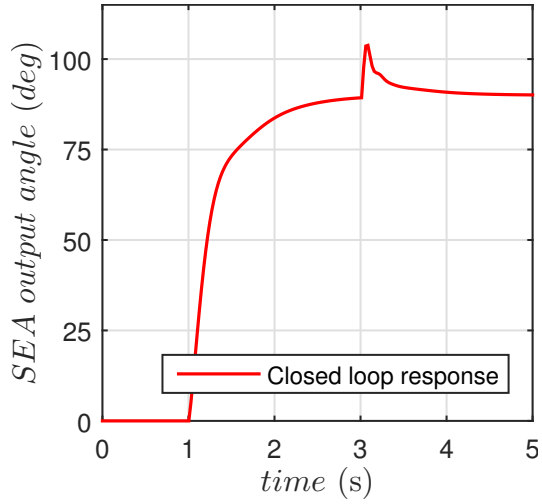

Fig. 16. Compensated system response showing how the closed loop SEA system is now capable of rejecting the same external disturbance.

4. CONCLUSION

This work presented a SEA upgrade solution based on an affordable module to be mounted to the output of an existing servo-motor. The two-part mechanical design was shown to be simple to manufacture, and the electronics circuit was designed around the popular Arduino platform, communicating angular displacements through the bus using the same infrastructure. We have also performed system identification and we have shown how robust position control can be achieved.

We are currently working on the final adjustments to allow experiments on real applications. For future work the authors also want to explore the use of torque mode control, available in the Dynamixel models MX-64 and MX-106.

ACKNOWLEDGEMENTS

Acknowledgements to the RoboCup Federation, Ostfalia University of Applied Sciences and to the Centro de Tecnologia of the Universidade Federal de Santa Maria for the funding support for this project.

REFERENCES

Carpino, G., Accoto, D., Sergi, F., Tagliamonte, N.L., and Guglielmelli, E. (2012). A novel compact torsional spring for series elastic actuators for assistive wearable robots. 134:121002, 1–10.

dos Santos, W.M. and Siqueira, A.A.G. (2014). Impedance control of a rotary series elastic actuator for knee rehabilitation. In *The International Federation of Automatic Control*, 4801–4806.

Guizzo, E. and Ackerman, E. (2012). The rise of the robot worker. *IEEE Spectrum*, 49(10), 34–41.

Hannemann, A.K., Stiddien, F., Xia, M., Krebs, O., Gerndt, R., Krupop, S., Bolze, T., and Lorenz, T. (2014). WF Wolves – Humanoid kid size team description for RoboCup 2014. RoboCup Tournament 2014. URL `http://www.wf-wolves.de`.

Jain, A. and Kemp, C.C. (2010). Pulling open doors and drawers: Coordinating an omni-directional base and a compliant arm with equilibrium point control. In *IEEE International Conference on Robotics and Automation (ICRA)*, 1807–1814.

Laffranchi, M., Sumioka, H., Sproewitz, A., Gan, D., and Tsagarakis, N. (2011). Compliant actuators. In *Adaptive Modular Architectures for Rich Motor Skills*.

Ljung, L. (1987). *System Identification: Theory for the User*. Prentice Hall, Englewood Cliffs, New Jersey.

Martins, L.T., de Mendonça Pretto, R., Gerndt, R., and da Silva Guerra, R. (2014). Design of a modular series elastic upgrade to a robotics actuator. In *RoboCup 2014: Robot Soccer World Cup XVIII*.

Pratt, G. and Williamson, M. (1995). Human robot interaction and cooperative robots. In *IEEE/RSJ International Conference on Intelligent Robots and Systems*, volume 1, 399 – 406.

Tsagarakis, N., Laffranchi, M., Vanderborght, B., and Caldwell, D. (2009). A compact soft actuator unit for small scale human friendly robots. In *IEEE International Conference on Robotics and Automation*, 4356–4362.

Wyeth, G. (2006). Control issues for velocity sourced series elastic actuators. In *Australasian Conference on Robotics and Automation*.

Yoon, S., S.Kang, S.Kim, Kim, Y., M.Kim, and Lee, C. (2003). Safe arm with mr-based passive compliant joints and visco-elastic covering for service robot applications. In *IEEE/RSJ International Conference on Intelligent Robots and Systems*, volume 3, 2191–2196.